Peer-reviewed version available at Nanomaterials 2018, 8, 470; doi:10.3390/nano8070470

Article

Effect of the sodium polyacrylate on the magnetite nanoparticles produced by green chemistry routes: Applicability in forward osmosis

Juan Zufia-Rivas [1], Puerto Morales [1] and Sabino Veintemillas-Verdaguer [1,*]

[1] Instituto de Ciencia de Materiales de Madrid, ICMM/ CSIC Sor Juana Inés de la Cruz 3, Cantoblanco 28049, Madrid, Spain

* Correspondence: sabino@icmm.csic.es; Tel.: +34-913-349-061

Abstract: Aqueous dispersions of magnetic nanocomposites have been proposed as draw electrolytes in forward osmosis. One possible approach for the production nanocomposites based on magnetite nanoparticles and sodium polyacrylate, is the synthesis of the magnetic iron oxide by coprecipitation or oxidative precipitation in presence of an excess of the polymer. In this work we explored the effect of the polymer proportion on the nanomaterials produced by these procedures. The materials obtained were compared s with the obtained by the coating of magnetite nanocrystals produced beforehand with the same polymer. The samples were characterized by chemical analysis, photon correlation spectroscopy, thermogravimetry, X-ray diffraction, infrared spectroscopy, transmission electron microscopy and magnetometry. The general trend observed is that part of the polymer is incorporated to the magnetic material during the synthesis heavily modifying its texture, with a drastic reduction of the particle size and magnetic response. The aqueous dispersions of the nanocomposites were highly stable with hydrodynamic size roughly independent on the polymer proportion. Their osmotic pressure proportional to the concentration of the polyelectrolyte, was similar than the generated by the equivalent amount of free polymer in the case of samples generated by oxidative precipitation and smaller in the case of samples generated by coprecipitation. Finally the possibilities of using these materials as draw electrolytes in forward osmosis will be briefly discussed.

Keywords: magnetic nanoparticles; sodium polyacrylate; nanocomposites; draw solutes; forward osmosis.

1. Introduction

Forward osmosis (FO) is considered a technology for water desalination and reuse of wastewater with great potential [1-4]. The forward osmosis process uses an electrolyte of high osmotic pressure to drive the water molecules through a membrane from the waste or sea water instead of the high pressure pumps used in the standard reverse osmosis (RO). The benefits of such process, apart from the pressure reduction that operates on the membrane [5] come essentially from the reduction of the energetic cost of FO process, which is highly dependent on the water flux and the recover feasibility of the draw solute from the permeated water [6]. The use of simple inorganic salts as draw solute in combination with water distillation to recover the solute was initially explored in spite of the high energetic cost of the distillation process [7], phosphates and organic molecules were also proposed due to their low reverse flux through the membrane [8-11].

Considering the microfiltration as the separation technique for recovering the solute with negligible reverse flux, the sodic salts of hydrophilic polymers such as polyacrylic acid (PAANa) [12] polyaspartic acid [13], poly 4-styrenesulphonic acid [14], EDTA[15] and dendrimers [16] have been tested. Colloidal dispersions of carbon dots heavily functionalized with carboxylates could be advantageously used in combination with microfiltration due to their bigger size and high osmotic pressure[17]. Thermoresponsive substances that are able to produce sols of high osmotic pressure spontaneously and split in two phases with small changes in temperature, could be advantageously used as draw solutes obtaining the water from the water rich phase. These substances could be polymers [18,19] ionic liquids [20] and microgels [21-23]. Among the proposed draw electrolytes, the magnetic nanoparticles (MNP) appear to be ideal given its recover facility from the diluted draw solution by means of a magnetic field. MNP's have no osmotic pressure and need to be functionalized with molecules that generate it. The functionalization molecules are often polyelectrolytes as PAANa [24,25], dextran [26], chitosan[27], copolymers poloyethylene oxide-polyacrylic acid [28], silanes [29]. The use of a hydrophilic polymer with thermoresponsive capacity in addition to the creation of osmotic pressure facilitate the magnetic separation changing the polymer conformation and was successfully employed [30,31]. In a recent review, the topic of the diverse draw solutes claimed to be good for FO was fully addressed [32]. In this paper as a difference from the majority of previous contributions were single systems with high osmolalities were proposed and tested by means of FO experiments, we will put the focus on the attainment of high magnetic response, in order to make easy the recovering and recycling of the MNP's, even that this will undoubtedly lead to a detriment of the osmotic pressure of the draw solute [32]. The objective is to determine the maximum osmotic pressure compatible with the minimum magnetic response needed for separation in the model system Fe_3O_4/PAANa. This approach requires the preparation of a wide range of magnetic nanocomposites (MNC) of magnetic nanoparticles of different sizes dispersed in (PAANa) characterize them and compare their osmolalities and magnetic properties. Keeping in mind the need of green chemical procedures cheap and easily scalable, we selected two synthesis methods in aqueous solution at low temperatures and in absence of surfactants or organic solvents, i.e. standard coprecipitation method starting from an Fe(III) and an Fe(II) salts [33] and oxidative precipitation starting from an Fe(II) salt able to produce the highest magnetically responsive magnetite nanoparticles of particle sizes among 20-50 nm [34] [35]. Nanocomposites were produced in one step by precipitation of the iron salt in the presence of PAANa, or in two steps process by subsequent coating of the previously prepared magnetite nanoparticles. The general picture obtained will inform about the real capability of FO in water remediation when the recovering of the treated water had to be done exclusively by magnetic forces.

2. Materials and Methods

2.1. Materials

Iron(III) chloride solution 45%, iron chloride tetrahydrate ≥ 99 %, iron (II) sulfate heptahydrate ≥ 99 %, iron(III) nitrate nonahydrate > 99.99%, sodium nitrate ≥ 99 %, sodium hydroxide ≥ 98%, potassium hydroxide >85%, potassium nitrate >99, nitric acid >65%, hydrochloric acid >37%, sulfuric acid 0.01M, ammonium hydroxide solution 28%, poly (sodium acrylate) PAANa Mw of 2100 Da and triethylene glycol (TREG) 99% were bought from Sigma Aldrich and used as received.

2.2. Synthesis of MNC and MNP

Two synthesis methods were used for the production the MNP: coprecipitation starting from an Fe(III) and an Fe(II) salts and oxidative precipitation starting from an Fe(II) salt. Two different approaches were followed for the production of NC: (1) Preparation of pure magnetite MNP and subsequent coating with PAANa (2): Preparation of MNP's in the presence of PAANa.

2.2.1.Coprecipitation

In the case of the two step process, magnetite nanoparticles were obtained by adding rapidly 75 mL of 25% NH_4OH to 0.5 L of an aqueous solution 0.175 M in $FeCl_3$ and 0.334 M in $FeCl_2$. After 5 min of stirring, the MNP were separated by magnetic decantation. In a second step the surface of the MNP was activated by acid treatment as follows [36]: 300 mL of 2 M HNO_3 were added to the decanted MNP, redispersed by stirring, the supernatant was removed after the magnetic sedimentation and the MNP were redispersed in 75 mL of 1 M $Fe(NO_3)_3$ and 130 mL of water, and the slurry was heated at 90 °C for 30 min. The MNP were recovered again by magnetic decantation, washed with 300 mL of 2 M HNO_3 one time and three times more with water to remove the excess of acid.

In the case of the one step process, the coprecipitation in the presence of PAANa was carried out by adding different amounts of solid PAANa (2-50 g) to the alkaline precipitant solution containing NH_4OH, $FeCl_3$ and $FeCl_2$. The mixing during the precipitation was helped with a high speed homogenizer Ultra-Turrax® T25 (10000rpm, disperser IKA 525N-25G-ST). No acid treatment was performed on these samples. The excess of reagents was removed by extensive dialysis (using a 10000 Da cut-off membrane) and the product in powder form was obtained by lyophilization.

1.2.2. Oxidative precipitation

In a glove box under nitrogen, two solutions were prepared using degassed water: (A) 2.12 g $NaNO_3$ with 0.7 g NaOH in 225 mL of water; and (B) 1.67 g of $FeSO_4.7H_2O$ in 25 mL H_2SO_4 0.01 M. The solution B was added fast to the solution A while stirring vigorously during 15 min (final concentration of reagents 0.024 M $FeSO_4$, 0.07 M NaOH, 0.1 M $NaNO_3$). The green rust initially formed was transferred to a double jacketed recipient in which up to 50 g of solid PAANa powder was placed beforehand. When the polymer was present, the mixture was homogenized by 1 min of Ultra-Turrax® under the same conditions than in the coprecipitation process. Immediately the liquid from the thermostat set at 90 ºC was pumped into the external jacket for fast heating of the slurry without stirring. When 90 °C were reached (15 min), the reactor was closed and the solution was kept at 90 °C for 24 h. After that, the suspension was cooled at room temperature, the solid was separated by magnetic decantation outside the glove box, and washed several times with distilled water. In the presence of PAANa, acetone addition is needed to promote the separation of the nanocomposite. Finally the final volume of 50 cc was extensively dialyzed using a 10000 Da cut-off membrane and the product in powder form was obtained by lyophilization.

2.2.3. Coating of MNP: A two-step process

MNC can be alternatively obtained by chemical reaction of PAANa and the bare MNP's at 280 ºC as follows [37]: 6 g of dry MNP's were dispersed with sonication for 5 min in 64 mL TREG and added to a slurry prepared beforehand by Ultra-Turrax® dispersion during 12 hr at 90 ºC of 6 g of PAANa in 400 ml TREG (or 800 mL of TREG/water 50% w/w). The black suspension was overhead stirred at 200 rpm and heated to 280 °C under nitrogen very slowly for control the foam formation and simultaneous distillation of excess of water. Finally the 280 ºC were maintained for 30 min under reflux, with a heavy stream of N_2. After cooling the mixture was precipitated with acetone and washed 3 times with water using magnetic separation. Finally the suspension was dialyzed and lyophilized.

2.3. Characterization of MNC's

The dry product was characterized by X-ray powder diffraction (XRD) to check the absence of secondary phases. Particle size was evaluated by the use of the Scherrer equation from the width of the XRD (D8 Advance, Bruker)peaks (d_{DRX}) and from the direct measurements on the TEM

micrographs (200 keV JEOL-2000 FXII) (d_{TEM}). The presence of PAANa adsorbed and the type of linking was assessed by infrared spectroscopy (FTIR) (spectrophotometer IFS 66V-S, Bruker) and thermogravimetric analysis (ATD/DSC/TG Q600, TA Instruments) was performed in air (up to 800 ºC at a scan rate of 10 º/min) The amount of PAANa was determined from the carbon content determined by elemental analysis CHNS/CHNO (EA) (CNHS Elemental Analyzer PERKIN ELMER 2400) and the iron content expressed as magnetite and obtained by chemical analysis of iron by ICP-OES (Plasma Emission Spectrometer ICP PERKIN ELMER mod. OPTIMA 2100 DV) . The magnetic properties of the nanocomposites in powder form were determined in a vibrating sample magnetometer (MagLab® VSM Oxford Instruments) at room temperature. The saturation magnetization (Ms) was evaluated by extrapolating to infinite field the experimental results obtained in the field range where the magnetization increases, and it can be described by a $1/H$ law and the magnetic susceptibility was evaluated as the slope of the linear dependence of the magnetization with the applied field at low fields. The hydrodynamic size of the aqueous dispersions was studied by Dynamic Light Scattering (DLS) (Nanosizer® ZS, Malvern) and the osmolality of the dispersions determined using a freezing point osmometer (model nº 3320 from Advanced Instruments).

3. Results and Discussion

3.1. Characterization of MNCs prepared by a two-step process

Uncoated MNP obtained by coprecipitation and oxidative precipitation were characterized in previous works and present mean diameter sizes of 11 nm and 30 nm respectively [38,39]. Although the polyacrylate coating developed in this work afforded stable aqueous colloids at pH around 7, the amount of coating material on the nanoparticles surface was very low, that is 6 % for the 11 nm MNP obtained by coprecipitation and 1% for the 30 nm MNP obtained by oxidative precipitation. According to that, the osmolalities attained by the dispersions at 33% wt concentration were 50 and 10 mOsm/Kg respectively. However, magnetic response of the samples, evaluated here from the saturation magnetization value at room temperature (Ms) was very high, that is 74 Am^2/Kg for the 11 nm sample and 80 Am^2/Kg for the 30 nm sample, suggesting that both particles could be easily separated by magnetic fields. Unfortunately, their low osmolalities drastically limit the use of these nanoparticle suspensions in FO processes.

3.2. Characterization of MNC's prepared by an one-step process

3.2.1. Samples prepared by coprecipitation in presence of PAANa

In figure 1a we present electron micrographs of two representative samples obtained in the presence of 2 g PAANa and 50 g of PAANa (samples C2 and C50) with mean particle sizes of 4.4 and 2.7 nm (TEM), respectively. The XRD diffraction patterns, chemical analysis and thermogravimetric curves (Figure 1b, c) confirm that the samples are magnetite/maghemite with Scherrer sizes of 4.4 and 3.1 nm respectively, and with a proportion of PAANa of 19.2 % and 77.0 % respectively. Unfortunately the magnetic properties of the samples are strongly affected by the PAANa content with an important reduction of the saturation magnetization down to 15-5 emu/g, which means a reduction of 80 % of the magnetization respect to particles prepared in absence of polymer (71 Am^2/Kg). A superparamagnetic behavior with zero coercivity and remamence magnetisation is observed at room temperature for all samples, which is in agreement with the small particle size (<5 nm)[40] .

Preprints (www.preprints.org) | NOT PEER-REVIEWED | Posted: 4 June 2018 doi:10.20944/preprints201806.0024.v1

Peer-reviewed version available at Nanomaterials 2018, 8, 470; doi:10.3390/nano8070470

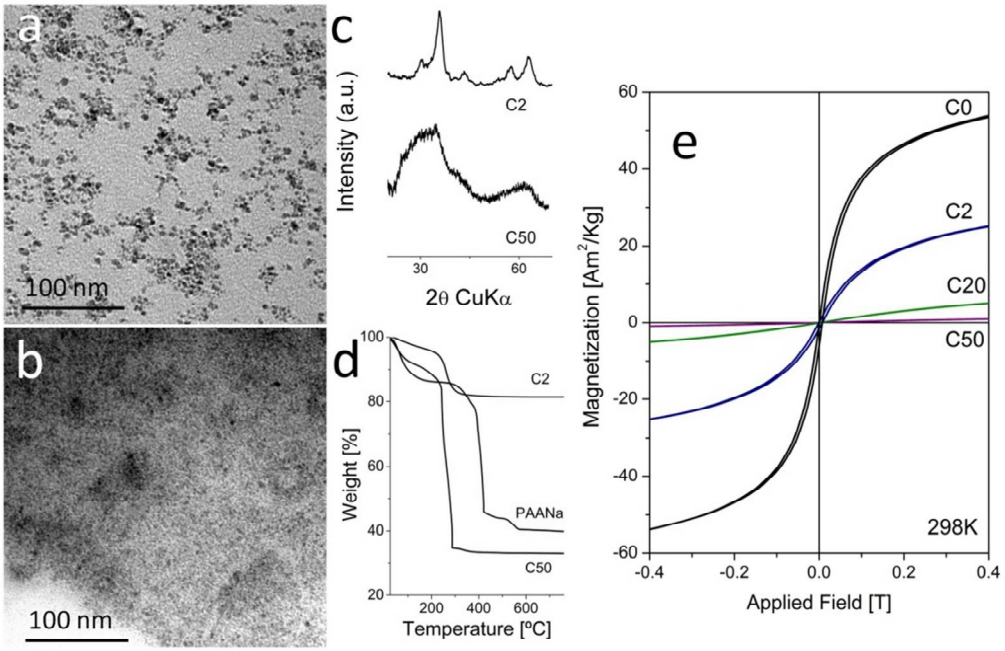

Figure 1. Characterization of MNC's produced by coprecipitation in one step. (a,b) TEM micrographs of C2 and C50, (c) Comparative XRD of samples C2 and C50 (d) Comparative TG of samples C2, C50 and pure PAANa, (e) Magnetization curves at room temperature.

3.2.2 Samples prepared by oxidative precipitation in presence of PAANa

In figure 2a we present electron micrographs of two representative samples obtained by oxidative precipitation in the presence of 10 g PAANa and 40 g of PAANa (samples OP10 and OP40) with average particle sizes going from around 28 nm to 4 nm (TEM), respectively. The XRD diffraction patterns (Figure 2b) chemical analysis and thermogravimetric curves (Figure 2c) confirm that the sample is magnetite/maghemite with Scherrer sizes of 34 and 5 nm respectively, and with a proportion of PAANa of 24.5 and 37.8 % respectively. It is remarkable the dramatic change in the nanostructure of the composites with the increase of the proportion of PAANa. Up to 20 g PAANa (mass ratio in the reactant mixture W_{PAANa}/W_{Fe} = 59) magnetite nanocrystals appeared in form of aggregates with the polymer among the individuals but above this limit magnetite nanocrystals appeared isolated and distributed evenly in the polymeric matrix (Figure 3).

The interaction among the PAANa and the magnetite nanocrystals were studied by infrared spectroscopy and analyzed using the principles established in ref [41]. The displacements of the carboxylate bands to lower wavenumbers, the increase of the difference among the symmetric and antisymmetric components with respect to the isolated PAANa and the predominance of the carbonyl band in high of PAANa composites is coherent with monodentate coordination. (Figure 4).

Peer-reviewed version available at Nanomaterials 2018, 8, 470; doi:10.3390/nano8070470

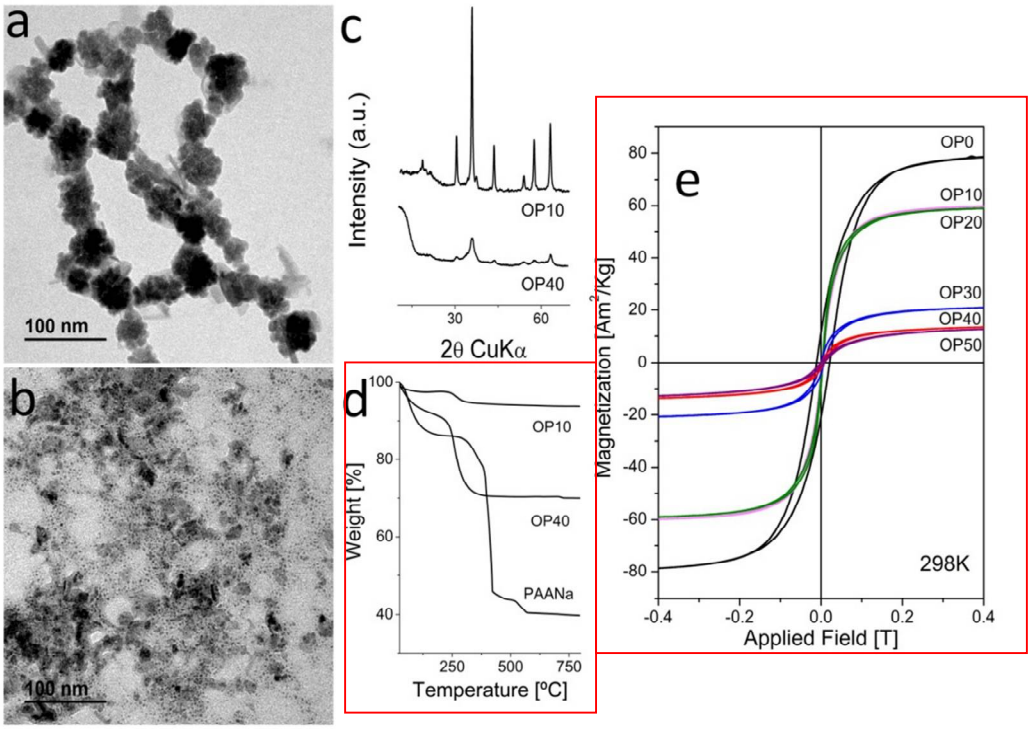

Figure 2. Characterization of MNC's produced by oxidative precipitation in one step. (a, b) TEM micrograph of OP10 and OP40, (c) Comparative XRD of samples OP10 and OP40, (d) Comparative TG of samples C10, C40 and pure PAANa , (e) Hysteresis cycles at room temperature.

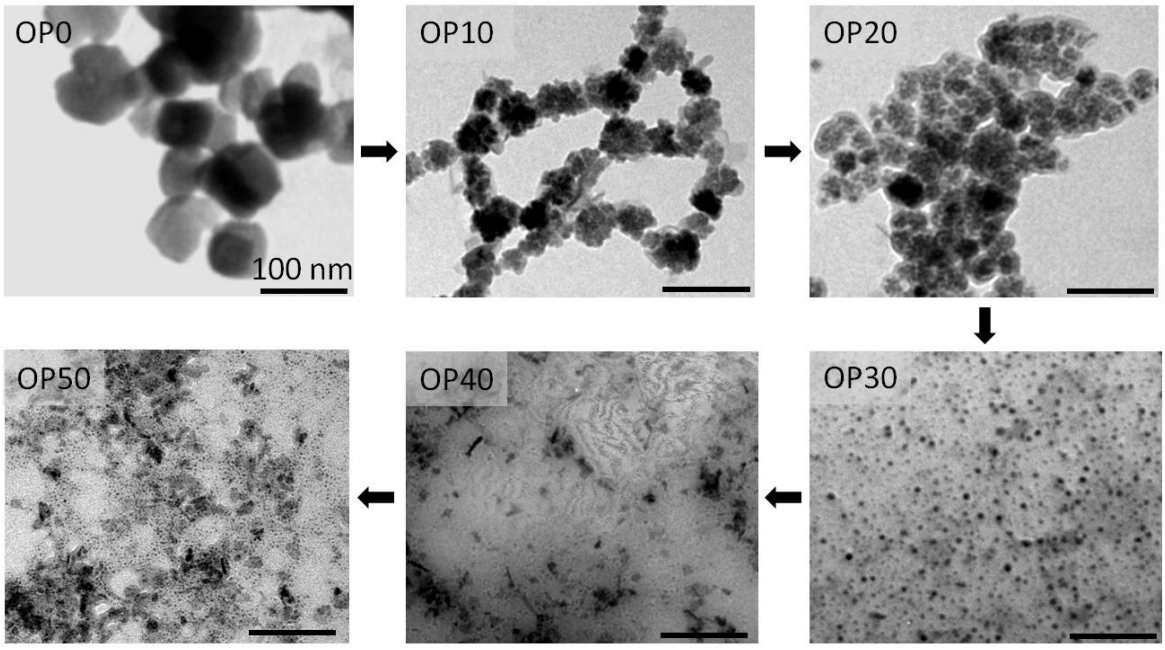

Figure 3. Evolution of the microstructures of MNC's obtained by oxidative precipitation as the proportion of PAANa increases.

As in the case of the samples prepared by coprecipitation, the saturation magnetization decreases strongly with the amount of PAANa from 120 Am^2/Kg down to 19 Am^2/Kg. The results of the

Preprints (www.preprints.org) | NOT PEER-REVIEWED | Posted: 4 June 2018 doi:10.20944/preprints201806.0024.v1

Peer-reviewed version available at Nanomaterials 2018, 8, 470; doi:10.3390/nano8070470

characterization of all samples produced in this work are summarized in Table 1. Interestingly, when we compare the saturation magnetization of the samples in Am^2/Kg Fe with reference magnetite samples of the same particle size we obtained good concordance except for sample OP30 (30 g PAANa) that presents a value abnormally low (Figure 1 and Table 1 Supplementary information). We hypothesize that in sample OP30 the polymer was somewhat incorporated in the structure of the magnetic material provoking the internal frustration of the spin interactions. Another indication of the intimate association of the polymer and the magnetite cores comes from the important shift of the decomposition temperature of the PAANa to lower temperatures in the composites with respect to the pure PAANa (Figures 1d, 2d and Figure 2 SI).
On the other hand, the coercivity is reduced to zero when the amount of polymer is higher than 30 % showing superparamagnetic behavior, according to the magnetic particle size reduction and probably the presence of the polymer reducing magnetic interactions inter-particles [40] . However, samples OP0, OP10 and OP20 have some residual coercivity that may result in higher tendency to aggregation in suspension and finally lack of colloidal stability.

Table 1. Results of the characterization of the MNC's obtained by coprecipitation and oxidative precipitation in one step. (d_{TEM}= Mean diameter by TEM; d_{DRX}= Mean crystal size by XRD; D_{HYD}=Hydrodynamic size in intensity (Z_{ave}) by DLS; Ms=Saturation magnetization; χ= Initial magnetic susceptibility).

Sample	d_{TEM} [nm]	d_{DRX} [nm]	D_{HYD} (Z_{ave}) [nm]	Fe_3O_4 ICP w%	PAANa EA w%	Ms 298K Am^2/Kg	χ 298K Am^2/KgT
C0	10±2	7.5	170	98	0	71	758
C2	4±1	4.4	95	74.0	19.2	43.4	192
C20	3±0.8	3.1	170	50.7	49.7	16.7	19
C50	3±1	3.3	170	21.7	77.0	5.6	4
OP0	50±20	67.3	560	98.7	0	82.5	*
OP10	28±5	34.2	270	72.9	4.5	63	1700
OP20	32±10	27.5	140	75.5	11.0	62	11900
OP30	7±1	10.9	150	53.0	31.0	24	463
OP40	4±1	4.9	220	52.6	27.0	20	219
OP50	3±0.6	5.4	170	41.1	51.5	19	186

(*) The sample OP0 is not superparamagnetic and the magnetic susceptibility is not defined

3.2.3 Osmolality and osmotic pressure as a function of the concentration

The values of the osmolalities measured as a function of the mass concentration up to the maximum practical concentration considering FO experiments (500g/L) and at a pH=8 to maximize the proportion of ionized $–COO^-$ groups in PAANa are presented in Figure 5a,b were it can be observed that the osmolalities increased linearly with the concentration for both sets of samples with slopes dependent on the PAANa content in the composite. The osmotic pressure is computed using the Van's Hoff expression (Equation 1).

$$\pi = cRT, \quad (1)$$

Where R=0.082 $atmL^{-1}K^{-1}Mol$. Were c was obtained from the experimental osmolality (m) measured with the freezing point osmometer, converted to molarities (c) using the expression (Equation 2) were d and C are the experimental density and mass concentration of the dispersion in g/cc.

$$c = m(d-C), \quad (2)$$

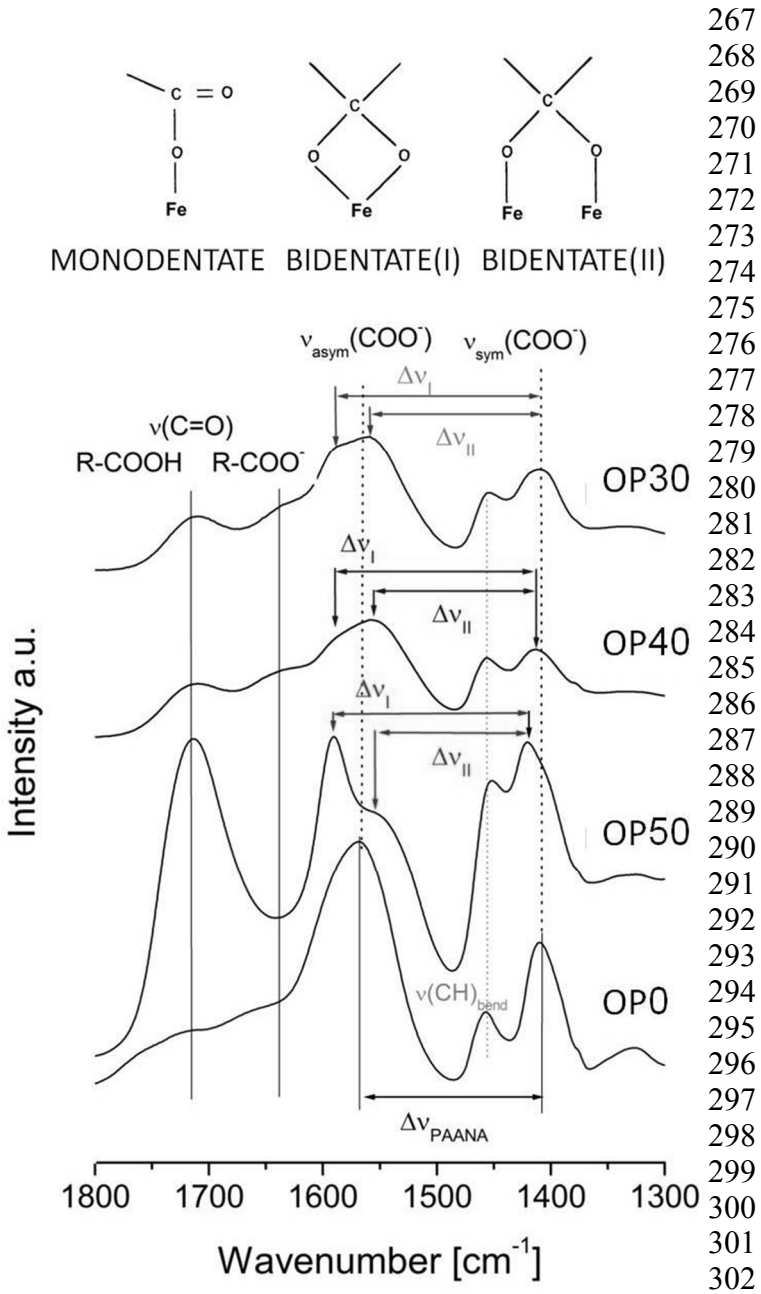

Figure 4. Infrared spectra of the MNC's obtained by oxidative precipitation. The evolution of the value of $\Delta\nu=\nu(COO^-)_{asym}-\nu(COO^-)_{sym}$ is presented. Monodentate coordination arises when $\Delta\nu > \Delta\nu_{PAANa}$ and exists ν(C=O), bidentate (I) when $\Delta\nu < \Delta\nu_{PAANa}$ and do not exist ν(C=O) and bidentate (III) $\Delta\nu \approx \Delta\nu_{PAANa}$ and exists ν(C=O).

In Figure 5c we present the evolution of the osmotic pressure with the PAANa concentration in the dispersion at the maximum concentration of composite (500g/L) for both sets of samples and the correspondent to the pure PAANa for comparison. . The osmotic pressure values attained in the Fe_3O_4/PAANa composites obtained by oxidative precipitation were similar than the ones produced by the PAANa alone, but those prepared by coprecipitation show a different trend that lead to lower osmotic pressures than the expected for their PAANa content. This fact could be originated by differences in the conformation of the polymer. Starting from the known tendency of polyelectrolytes to lay planar when adsorbed on polar surfaces [42]. We hypothesize that PAANa adsorbed during the coprecipitation of magnetite follow this trend, and the onion-like structure formed generate smaller osmotic pressures than the free polymer whereas, perhaps due to the

Preprints (www.preprints.org) | NOT PEER-REVIEWED | Posted: 4 June 2018 doi:10.20944/preprints201806.0024.v1

Peer-reviewed version available at Nanomaterials 2018, 8, 470; doi:10.3390/nano8070470

higher temperature of the synthesis of the oxidative precipitation, the PAANa adsorbed destabilize the planar configuration in favor to more open configurations (similar than the adopted by free PAANa in solution), more effective in the interaction with water.

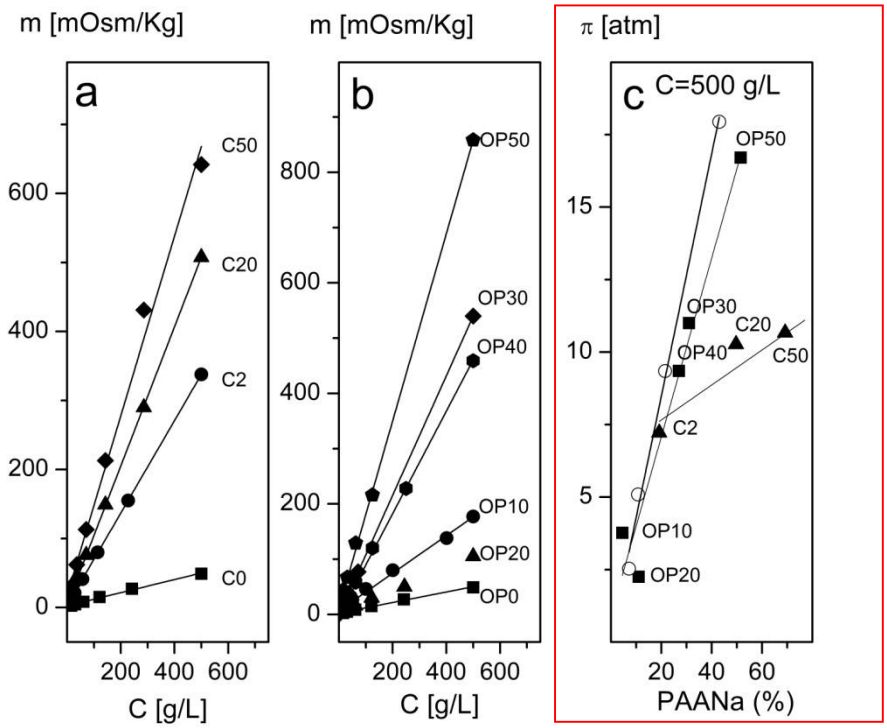

Figure 5. Variation of the osmolality with the concentration for samples of MNC's prepared by coprecipitation (a) and oxidative precipitation (b) in one step measured at room temperature and pH=8. In (c) we present the evolution of the osmotic pressure with the proportion of PAANa for all the samples, the results obtained by equivalent aqueous solutions of pure PAANa are presented for comparison (open circles).

3.2.4. Magnetic response

The magnetic response of a colloidal system formed by magnetic nanoparticles, in the concentration range needed for its use as draw electrolyte, is difficult to predict due to the magnetic interactions that tend to reduce the effective field with respect to the input field [43] and the effect of the aggregation that favors the cooperation among the magnetic cores. Particles with sufficient high moment may form clusters with different configurations such as chains, loops or anisometric aggregates that will modify its magnetic response but they will not be considered here. In any case the magnetic energy (E) and the magnetic force (F) are given by the expressions (Equations.3, 4) [44].

$$E=\mu_0 mH, \quad (3)$$

$$F=\mu_0 mH\nabla H, \quad (4)$$

Where $\mu_0=1.2566\cdot10^{-6}$ $VsA^{-1}m^{-1}$ is the permeability of free space, m is the magnetization of the colloidal aggregate of Fe_2O_3/PAANa nanoparticles in the aqueous dispersion and (H) is the magnetic field. The key parameter is the maximum magnetization attained by the aggregate that will depend on the aggregate size and the saturation magnetization. The aggregate size of the colloids is approximately independent on the particle size (Table 1), being in the range of 150-200 nm (with the exception of the uncoated particles OP0) what assures stability at neutral pH. Therefore, the only parameter important to distinguish the magnetic response of the composites is the saturation magnetization (m_s) of a single MNP coated with PAANa (Equation 5).

Preprints (www.preprints.org) | NOT PEER-REVIEWED | Posted: 4 June 2018 doi:10.20944/preprints201806.0024.v1

Peer-reviewed version available at Nanomaterials 2018, 8, 470; doi:10.3390/nano8070470

$$m_s = \frac{4}{3}\pi\left(\frac{d_{DRX}\cdot 10^{-9}}{2}\right)^3 d_{Fe3O4}\cdot\left(1+\frac{PAANa}{100\text{-}PAANa}\right)\cdot M_s, \quad (5)$$

were ρ_{Fe3O4} is the density of the MNP approximated to the magnetite value 5200 Kg/m^3. Figure 6 presents the logarithm of m_s as a function of the particle size. From the linear dependence obtained (with the exception of the smaller nanoparticles that give smaller response due to surface spin canting [40]) it can be seen that the magnetic response drops logarithmically with the reduction of particle size, independently of the method of synthesis and the proportion of PAANa .

The osmolality also displayed in the Figure 6 shows much higher values for the smaller nanoparticles due to the higher proportion of PAANa but with much more scattering depending on the synthesis conditions. The dependence with the particle size seems to be approximately linear with a steeper decay for the coprecipitation method.

In general terms the results of osmotic pressures and magnetizations presented compare well with previous studies using the same nanocomposites obtained by other methods [45] [46]. The advantages of the application of oxidative precipitation to the preparation of draw solutes presented here come from the simplicity of their preparation, the scalability of the process and the possibility to obtain a range of osmolalities and magnetic responses by simply changing the proportion of PAANa in the reaction media.

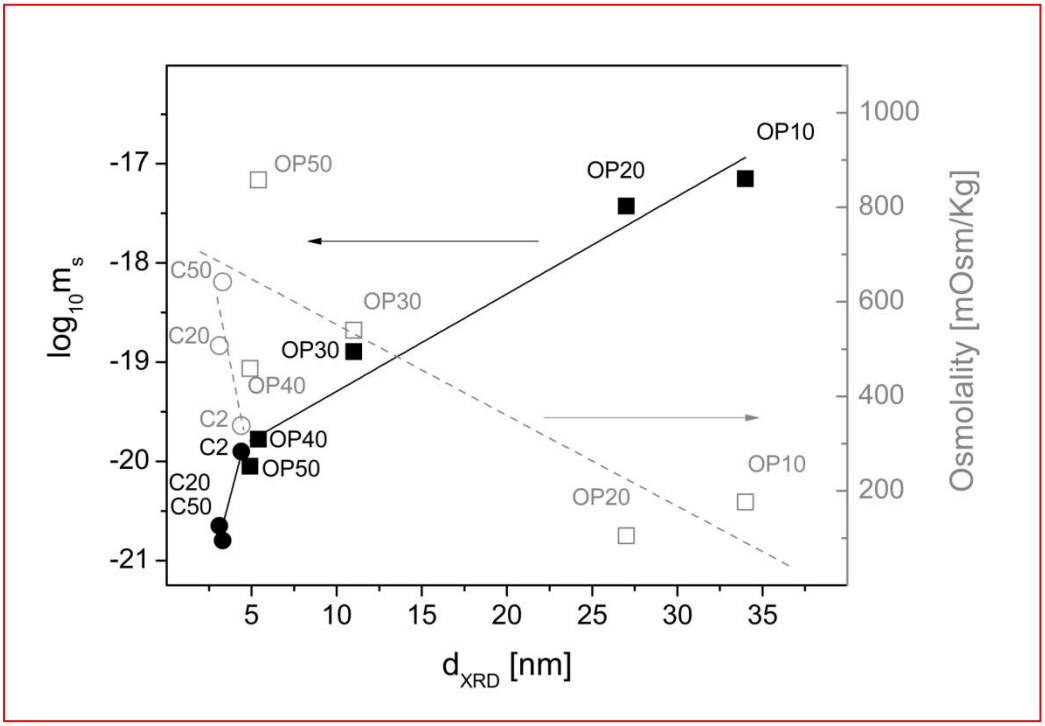

Figure 6. Dependence of the magnetic response and the osmolality of MNC's as a function of the particle size obtained from the XRD data. Full square points (■) represent the magnetic response of samples produced by oxidative precipitation. Full round points (●) represent the magnetic response of samples produced by coprecipitation. Empty squarepoints (□) represent the osmolality for samples produced by oxidative precipitation and empty round points (○) the osmolality for samples produced by coprecipitation, in both cases at 500 g/L.

4. Conclusions

The main conclusion attained in this work is that in order to obtain high magnetic response and high osmolality in nanocomposites based on magnetite nanoparticles and PAANa, one pot synthesis is the best strategy. The multistep procedure could successfully functionalize highly responsive magnetic nanoparticles with low coating densities insufficient to reach high osmotic pressure in a scalable cost effective way. The single pot procedure imposes the presence of the polymer on the nanoparticle surface that is responsible for the osmotic pressure in such amount that impedes the growth of the magnetic cores, in detriment of the magnetic performance. This limitation imposes the need of adjust the experimental conditions of synthesis in order to achieve a compromise for both properties for the particular application envisaged. In this work we found that best compromise solution for the system Fe_3O_4/PAANa was the nanocomposite OP30 that presents at the same time good magnetic response, > 25 Am^2/Kg, superparamagnetic and therefore reversible behavior and relatively high osmotic pressure, 11 bar at high concentration. Such draw electrolyte, provided that the PAANa could resist the harsh conditions of repetitive FO processes, could be useful in certain FO applications dealing with polluted continental or waste waters.

Supplementary Materials: The following are available online at www.mdpi.com/link, Figure S1. Hysteresis cycles of Fe_3O_4/PAANa nanocomposites obtained by oxidative precipitation expressed in Am^2/Kg Fe, Table S1. Comparison of the saturation magnetization per Kg of iron present in the composite samples of Fe_3O_4/PAANa obtained by oxidative precipitation with the reference samples of pure magnetite/maghemite of similar size, Figure S2. Thermogravimetric analysis of all samples showing the shift in the decomposition temperature of adsorbed PAANa

Acknowledgments: A This work was supported by the Spanish Ministry of Economy and Competitiveness, N◦ MAT2017-88148-R and for several research contracts with Jayim Mayim S.L. Special thanks are given to Mrs. Cristina Marsans Astoreca (Jayim Mayim S.L.) who gave us the initial impulse to work in the desalination problem. Costs to publish in open access are allowed by our funding institution.

Author Contributions: J.Z. performed the experiments, S.V. conceived and designed the experiments; P.M. analyzed the data; S.V. wrote the paper.

Conflicts of Interest: The authors declare no conflict of interest.

References

1. Klaysom, C.; Cath, T.Y.; Depuydt, T.; Vankelecom, I.F.J. Forward and pressure retarded osmosis: Potential solutions for global challenges in energy and water supply. *Chemical Society Reviews* **2013**, *42*, 6959-6989.
2. McGovern, R.K.; Lienhard, J.H. On the potential of forward osmosis to energetically outperform reverse osmosis desalination. *Journal of Membrane Science* **2014**, *469*, 245-250.
3. Valladares Linares, R.; Li, Z.; Sarp, S.; Bucs, S.S.; Amy, G.; Vrouwenvelder, J.S. Forward osmosis niches in seawater desalination and wastewater reuse. *Water research* **2014**, *66*, 122-139.

4. Qasim, M.; Darwish, N.A.; Sarp, S.; Hilal, N. Water desalination by forward (direct) osmosis phenomenon: A comprehensive review. *Desalination* **2015**, *374*, 47-69.
5. Akther, N.; Sodiq, A.; Giwa, A.; Daer, S.; Arafat, H.A.; Hasan, S.W. Recent advancements in forward osmosis desalination: A review. *Chemical Engineering Journal* **2015**, *281*, 502-522.
6. Cai, Y.; Hu, X.M. A critical review on draw solutes development for forward osmosis. *Desalination* **2016**, *391*, 16-29.
7. Achilli, A.; Cath, T.Y.; Childress, A.E. Selection of inorganic-based draw solutions for forward osmosis applications. *Journal of Membrane Science* **2010**, *364*, 233-241.
8. Hau Thi, N.; Chen, S.-S.; Nguyen Cong, N.; Huu Hao, N.; Guo, W.; Li, C.-W. Exploring an innovative surfactant and phosphate-based draw solution for forward osmosis desalination. *Journal of Membrane Science* **2015**, *489*, 212-219.
9. Long, Q.W.; Wang, Y. Sodium tetraethylenepentamine heptaacetate as novel draw solute for forward osmosis-synthesis, application and recovery. *Energies* **2015**, *8*, 12917-12928.
10. Long, Q.; Qi, G.; Wang, Y. Synthesis and application of ethylenediamine tetrapropionic salt as a novel draw solute for forward osmosis application. *Aiche Journal* **2015**, *61*, 1309-1321.
11. Nguyen Cong, N.; Hau Thi, N.; Ho, S.-T.; Chen, S.-S.; Huu Hao, N.; Guo, W.; Ray, S.S.; Hsu, H.-T. Exploring high charge of phosphate as new draw solute in a forward osmosis-membrane distillation hybrid system for concentrating high-nutrient sludge. *Science of the Total Environment* **2016**, *557*, 44-50.
12. Ge, Q.; Su, J.; Amy, G.L.; Chung, T.-S. Exploration of polyelectrolytes as draw solutes in forward osmosis processes. *Water Research* **2012**, *46*, 1318-1326.
13. Gwak, G.; Jung, B.; Han, S.; Hong, S. Evaluation of poly (aspartic acid sodium salt) as a draw solute for forward osmosis. *Water Research* **2015**, *80*, 294-305.
14. Tian, E.; Hu, C.; Qin, Y.; Ren, Y.; Wang, X.; Wang, X.; Xiao, P.; Yang, X. A study of poly (sodium 4-styrenesulfonate) as draw solute in forward osmosis. *Desalination* **2015**, *360*, 130-137.
15. Nguyen Thi, H.; Chen, S.-S.; Nguyen Cong, N.; Huang, K.Z.; Huu Hao, N.; Guo, W. Exploration of edta sodium salt as novel draw solution in forward osmosis process for dewatering of high nutrient sludge. *Journal of Membrane Science* **2014**, *455*, 305-311.
16. Zhao, D.; Chen, S.; Wang, P.; Zhao, Q.; Lu, X. A dendrimer-based forward osmosis draw solute for seawater desalination. *Industrial & Engineering Chemistry Research* **2014**, *53*, 16170-16175.
17. Guo, C.X.; Zhao, D.; Zhao, Q.; Wang, P.; Lu, X. Na+-functionalized carbon quantum dots: A new draw solute in forward osmosis for seawater desalination. *Chemical Communications* **2014**, *50*, 7318-7321.
18. Zhao, D.; Wang, P.; Zhao, Q.; Chen, N.; Lu, X. Thermoresponsive copolymer-based draw solution for seawater desalination in a combined process of forward osmosis and membrane distillation. *Desalination* **2014**, *348*, 26-32.
19. Kim, J.-J.; Kang, H.; Choi, Y.-S.; Yu, Y.A.; Lee, J.-C. Thermo-responsive oligomeric poly(tetrabutylphosphonium styrenesulfonate)s as draw solutes for forward osmosis (fo) applications. *Desalination* **2016**, *381*, 84-94.

20. Zhong, Y.; Feng, X.; Chen, W.; Wang, X.; Huang, K.-W.; Gnanou, Y.; Lai, Z. Using ucst ionic liquid as a draw solute in forward osmosis to treat high-salinity water. *Environmental Science & Technology* **2016**, *50*, 1039-1045.
21. Hartanto, Y.; Zargar, M.; Wang, H.; Jin, B.; Dai, S. Thermoresponsive acidic microgels as functional draw agents for forward osmosis desalination. *Environmental Science & Technology* **2016**, *50*, 4221-4228.
22. Hartanto, Y.; Zargar, M.; Cui, X.; Shen, Y.; Jin, B.; Dai, S. Thermoresponsive cationic copolymer microgels as high performance draw agents in forward osmosis desalination. *Journal of Membrane Science* **2016**, *518*, 273-281.
23. Wei, J.; Low, Z.-X.; Ou, R.; Simon, G.P.; Wang, H. Hydrogel-polyurethane interpenetrating network material as an advanced draw agent for forward osmosis process. *Water Research* **2016**, *96*, 292-298.
24. Dey, P.; Izake, E.L. Magnetic nanoparticles boosting the osmotic efficiency of a polymeric fo draw agent: Effect of polymer conformation. *Desalination* **2015**, *373*, 79-85.
25. Ling, M.M.; Wang, K.Y.; Chung, T.-S. Highly water-soluble magnetic nanoparticles as novel draw solutes in forward osmosis for water reuse. *Industrial & Engineering Chemistry Research* **2010**, *49*, 5869-5876.
26. Bai, H.; Liu, Z.; Sun, D.D. Highly water soluble and recovered dextran coated fe3o4 magnetic nanoparticles for brackish water desalination. *Separation and Purification Technology* **2011**, *81*, 392-399.
27. Shabani, Z.; Rahimpour, A. Chitosan- and dehydroascorbic acid-coated fe3o4 nanoparticles: Preparation, characterization and their potential as draw solute in forward osmosis process. *Iranian Polymer Journal* **2016**, *25*, 887-895.
28. Bai, J.; Wang, X.; Fu, P.; Cui, Z.; Zhao, Q.; Pang, X.; Liu, M. Highly water-dispersed superparamagnetic magnetite colloidal nanocrystal clusters from multifunctional polymeric nanoreactors: Synthesis and properties. *Rsc Advances* **2016**, *6*, 9429-9435.
29. Park, S.Y.; Ahn, H.-W.; Chung, J.W.; Kwak, S.-Y. Magnetic core-hydrophilic shell nanosphere as stability-enhanced draw solute for forward osmosis (fo) application. *Desalination* **2016**, *397*, 22-29.
30. Zhao, Q.; Chen, N.; Zhao, D.; Lu, X. Thermoresponsive magnetic nanoparticles for seawater desalination. *Acs Applied Materials & Interfaces* **2013**, *5*, 11453-11461.
31. Ling, M.M.; Chung, T.-S.; Lu, X. Facile synthesis of thermosensitive magnetic nanoparticles as "smart" draw solutes in forward osmosis. *Chemical Communications* **2011**, *47*, 10788-10790.
32. Zhao, D.; Chen, S.; Guo, C.X.; Zhao, Q.; Lu, X. Multi-functional forward osmosis draw solutes for seawater desalination. *Chinese Journal of Chemical Engineering* **2016**, *24*, 23-30.
33. Bee, A.; Massart, R.; Neveu, S. Synthesis of very fine maghemite particles. *Journal of Magnetism and Magnetic Materials* **1995**, *149*, 6-9.
34. Sugimoto, T.; Matijevic, E. Formation of uniform spherical magnetite particles by crystallization from ferrous hydroxide gels. *Journal of Colloid and Interface Science* **1980**, *74*, 227-243.
35. Andres Verges, M.; Costo, R.; Roca, A.G.; Marco, J.F.; Goya, G.F.; Serna, C.J.; Morales, M.P. Uniform and water stable magnetite nanoparticles with diameters around the monodomain-multidomain limit. *Journal of Physics D-Applied Physics* **2008**, *41*.

36. Costo, R. Synthesis and characterization of ultrasmall iron oxide magnetic colloids for biomedical applications. Autonomous University of Madrid, Madrid, 2010.
37. Veintemillas, V.S.; Morales, H.M.P.; Serna, P.C.; Marsans, A.C.; Lopez, H.V. Electrolito nanoestructurado útil para desalinización por osmosis directa, procedimiento de obtención del electrolito y usos del mismo. 2015.
38. Costo, R.; Bello, V.; Robic, C.; Port, M.; Marco, J.F.; Puerto Morales, M.; Veintemillas-Verdaguer, S. Ultrasmall iron oxide nanoparticles for biomedical applications: Improving the colloidal and magnetic properties. *Langmuir* **2012**, *28*, 178-185.
39. Luengo, Y.; Morales, M.P.; Gutierrez, L.; Veintemillas-Verdaguer, S. Counterion and solvent effects on the size of magnetite nanocrystals obtained by oxidative precipitation. *Journal of Materials Chemistry C* **2016**, *4*, 9482-9488.
40. Morales, M.P.; Veintemillas-Verdaguer, S.; Montero, M.I.; Serna, C.J.; Roig, A.; Casas, L.; Martinez, B.; Sandiumenge, F. Surface and internal spin canting in gamma-fe2o3 nanoparticles. *Chemistry of Materials* **1999**, *11*, 3058-3064.
41. Jones, F.; Farrow, J.B.; van Bronswijk, W. An infrared study of a polyacrylate flocculant adsorbed on hematite. *Langmuir* **1998**, *14*, 6512-6517.
42. Bremmell, K.E.; Scales, P.J. Adhesive forces between adsorbed anionic polyelectrolyte layers in high ionic strength solutions. *Colloids and Surfaces a-Physicochemical and Engineering Aspects* **2004**, *247*, 19-25.
43. de la Presa, P.; Luengo, Y.; Velasco, V.; Morales, M.P.; Iglesias, M.; Veintemillas-Verdaguer, S.; Crespo, P.; Hernando, A. Particle interactions in liquid magnetic colloids by zero field cooled measurements: Effects on heating efficiency. *Journal of Physical Chemistry C* **2015**, *119*, 11022-11030.
44. Odenbach, S. Chapter 3 ferrofluids. In *Handbook of Magnetic Materials*, 2006; Vol. 16, pp 127-208.
45. Ling, M.M.; Chung, T.-S. Desalination process using super hydrophilic nanoparticles via forward osmosis integrated with ultrafiltration regeneration. *Desalination* **2011**, *278*, 194-202.
46. Mino, Y.; Ogawa, D.; Matsuyama, H. Functional magnetic particles providing osmotic pressure as reusable draw solutes in forward osmosis membrane process. *Advanced Powder Technology* **2016**, *27*, 2136-2144.

552

553 **SUPPLEMENTARY INFORMATION**

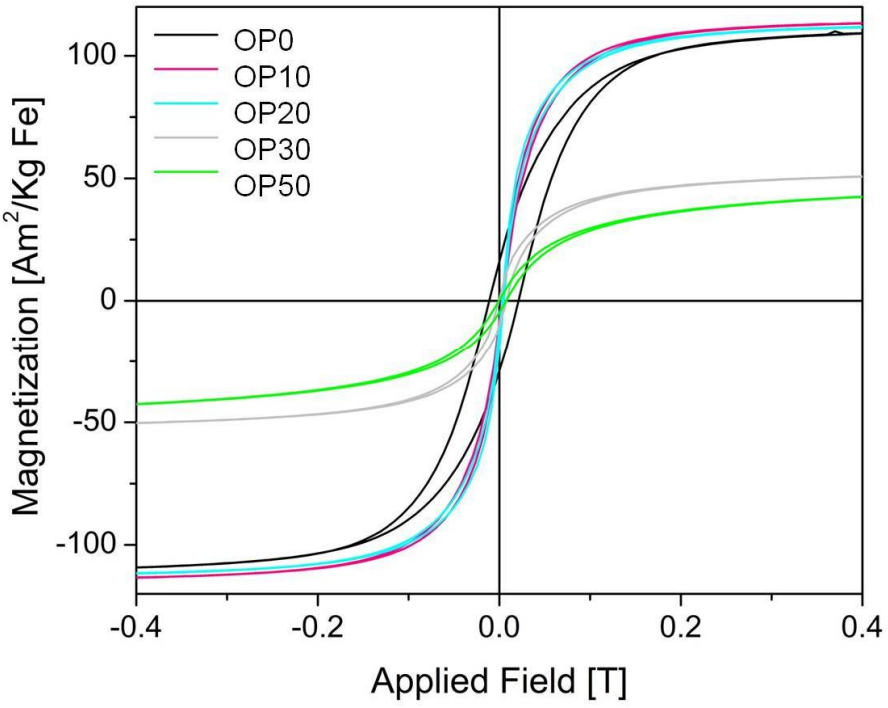

FIGURE 1 (SI)

554

555 **Figure S1 Hysteresis cycles of selected samples. Magnetization is normalized to the mass of iron.**

556 **TABLE S1**

557 **Saturation magnetization and magnetic susceptibilities of selected samples normalized to iron**
558 **content and comparison with the samples of pure magnetite of the same size**

SAMPLE	$D_{SHERRER}$ nm	Ms (Fe) Am²/KgFe 298 K	γ (Fe) Am²/KgFeT 298 K	Pure samples as reference	
				Size [nm]	Ms(Fe) Am²/KgFe 298 K
OP10	34	120.0 ± 0.4	3170 ± 178	*35*	120
OP20	27	117.8 ± 0.3	3094 ± 157	*25*	114
OP30	11	**63.8** ± 0.2	1205 ± 197	*10*	**86**
OP50	5	63.8 ± 0.2	636 ± 70	*5*	56

559

Peer-reviewed version available at Nanomaterials 2018, 8, 470; doi:10.3390/nano8070470

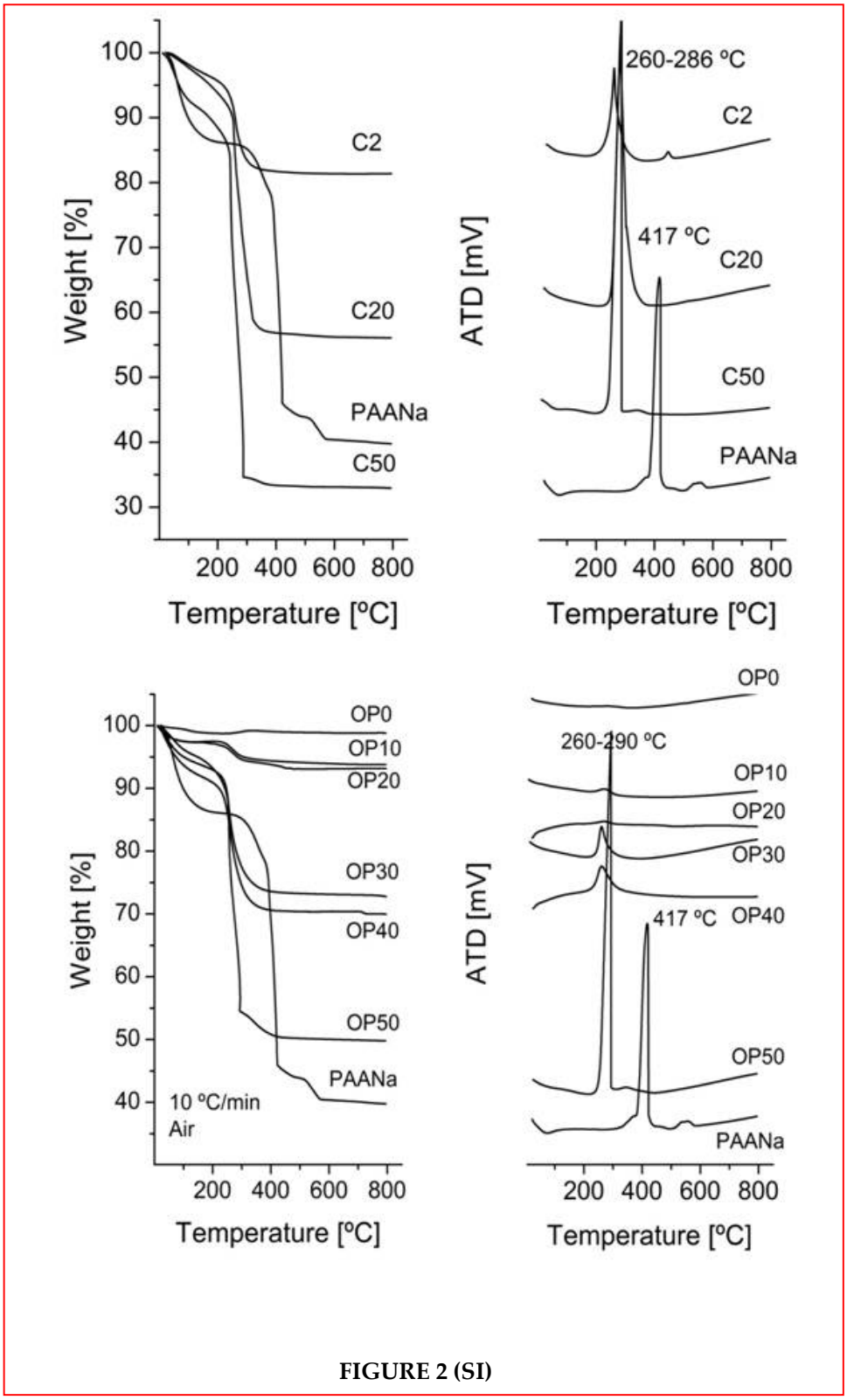

FIGURE 2 (SI)

Figure S2. TG-ATD curves of all the samples of this study in comparison of the given by pure PAANa